PRELIMINARY OBSERVATIONS ON THE RELATIONSHIP BETWEEN FE-SIGNATURES AND PSR LOCATIONS AT THE LUNAR SOUTH POLE. C. J. Ahrens[1], N. Petro[1], S. Li[2], [1]NASA Goddard Space Flight Center, Solar System Exploration Division, Greenbelt, MD (Caitlin.ahrens@nasa.gov), [2]Hawai'i Institute of Geophysics and Planetology, University of Hawaii, Honolulu, HI.

Introduction: Volatiles are observed at several lunar polar craters, particularly the permanently shadowed regions (PSRs). Recent observations have shown certain craters appear to have asymmetries in potential ice deposits as well as variation of temperatures based on measurements from Lunar Reconnaissance Orbiter's Lunar Orbiter Laser Altimeter (LRO-LOLA), Diviner Lunar Radiometer Experiment (Diviner), and Moon Mineralogy Mapper (M3).

Hayne et al. [1] found that many PSR's near the lunar south pole have maximum surface temperatures < 100 K, consistent with the presence of stable water ice found using LRO's Lyman Alpha Mapping Project (LAMP) [2]. Surface temperatures in these shadowed regions are largely controlled by reflected sunlight and irradiated infrared light from adjacent topography [3-6]. These areas act as cold traps, capable of accumulating water and other volatile compounds over time [7]. However, surfaces that experience temperatures > 100 K should lack surface water ice due to the temperature-dependent sublimation [8]. Conversely, surfaces within < 100 K temperature conditions can preserve surface frost over geological time periods.

The lunar surface and interior are highly reducing, where metallic iron (as an igneous phase) is found in lunar basalts [9, 10]. The lack of a lunar atmosphere allows solar wind to reach the lunar surface and be implanted into the top layer of surface grains (tens to hundreds to nanometers) [11]. Li et al. [9] states that the lunar poles harboring water ice could lead to observations regarding the possibility of alternation due to mineral contact with ice [12] or sublimation vapor from the ice [13]. With FeO-mineralogy on the Moon, namely at the lunar highlands and mare regions [14], higher FeO wt% has been correlated to clinopyroxene/high-Ca-Al pyroxenes while lower concentrations of FeO correspond to orthopyroxene/low-Ca-Al pyroxenes [14]. It should be noted that Ca and Al-bearing rocks have a higher thermal conductivity than Fe and Mg-bearing rocks [15].

There is a current lack of understanding regarding the thermal stability of these PSRs. In this preliminary work, we measure the day and night-time bolometric temperatures from Diviner over three years (2009-2011). From these changes in day-night temperatures, we can observe that PSR temperatures are highly variable in relation to the crater rim temperatures, especially craters that have a higher concentration of FeO-type materials. We identified five craters in the south pole with this trend but display two example craters with different FeO abundances for this abstract.

Methodology: LROC Wide Angle Camera (WAC) and Diviner data were used, all publicly available on the Planetary Data System (PDS) Geosciences Node, together with the Java Mission-planning and Analysis for Remote Sensing (JMARS) software. Coincident Diviner temperature data was available at a resolution of 500 m [16]. Four temperatures (day and night) were taken at each crater site and averaged for each year (2009-2011).

A combination of Clementine data (using the ultraviolet-visible camera – UVVIS) [14] and Moon Mineralogy Mapper observations from [9], we chose candidate craters that had a PSR observation (verified using the LROC Quickmap) and FeO signatures.

Results: *Kocher* (84.74°S, 134.02°W): This crater is estimated to have ~18 wt% FeO (Figure 1A) from Lunar Prospector data. The averaged Diviner temperatures over the three-year timespan (Figure 1B) shows that the crater rim/walls and the PSR (outlined in Figure 1A, C, D) temperature at night remain the highest and lowest temperatures, as to be expected. However, the PSR temperatures during the day (blue line in Figure 1B, Figure 1C) show that this area is unusually high for a volatile coldtrap (100 – 140 K). Moreso, the crater rim/wall is similar, if not slightly colder than the PSR at night (gold line in Figure 1B, Figure 1D).

de Gerlache (88.48°S, 88.34°W): This crater is observed to have < 8 wt% FeO (Figure 2A). The measured averaged Diviner temperatures (Figure 1B) reveal that the crater rim/walls and the PSR (outlined in Figure 1A, C, D) temperature at night are similar to those at Kocher crater. However, the PSR temperatures during the day (blue line in Figure 1B, Figure 1C) show that this area is lower in temperature (~65 K) compared not only to the crater rim/wall at night (Figure 2D) but also at Kocher crater.

Discussion: We find that temperature variations associated with the PSR volatiles and observed FeO signatures at certain craters can reveal a relationship on the apparent influence of mineralogy stability. By understanding that higher concentrations of FeO-minerals have higher thermal conductivity, this in turn can influence the thermal capacity of the volatile ices (i.e., retain residual thermal diffusivities from the FeO-bearing crater wall/rim). Thus, the continuation of this work could potentially address key questions for lunar exploration, especially the perspective on cold trapping processes, volatile distribution at the poles, and regolith properties, all of which are outlined in the Planetary Science Decadal Survey, Visions and Voyages [17].

Acknowledgments: This research was supported by an appointment to the NASA Postdoctoral Program at the NASA Goddard Space Flight Center, administered by Universities Space Research Association under contract with NASA.

References: [1] Hayne, P., et al. (2015) Icarus, 255, 58-69. [2] Gladstone, G.R., et al. (2010) Space Sci. Rev.150(1-4), 161–181. [3] Watson, K., et al. (1961) J Geophys. Res., 66, 3033-3045. [4] Ingersoll, A., et al. (1992) Icarus, 100, 40-47. [5] Salvail, J., Fanale, F., (1994) Icarus, 111, 441-455. [6] Vasavada, A., et al. (1999) Icarus, 141, 179-193. [7] Li, S., et al., (2018) PNAS, 115 (36), 8907-8912. [8] Andreas, E., (2007) Icarus, 186 (1), 24-30. [9] Li, S., et al. (2020) Sci. Adv., 6, eaba1940. [10] G. J. Taylor, et al. (1991) Lunar rocks, in Lunar Source Book, Cambridge Univ. Press, pp. 183–284. [11] Hapke, B. (2001) JGR Planets, 106, 10039-10073. [12] Cocks, F., et al. (2002) Icarus, 160, 386-397. [13] Stopar, J., et al. (2018) Planet Space Sci., 162, 157-169. [14] Lucey, P., Blewett, D., Jolliff, B. (2000) JGR, 105 (E8), 20297-20305. [15] Engineeringtoolbox.com. [16] Chin, G., et al. (2007) Space Sci. Rev., 129 (4), 391-419. [17] NRC (2011).

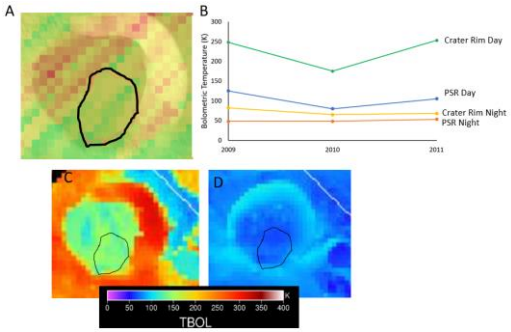

Figure 1: Kocher crater with PSR outlined in black. A) LOLA albedo overlain on LROC imaging. B) Averaged Diviner data from 2009-2011 (Green – Crater rim/wall temperature; Blue – PSR Daytime; Gold – Crater rim/wall; Red – PSR Nighttime). C) Daytime bolometric temperature from Diviner. D) Nighttime bolometric temperature from Diviner.

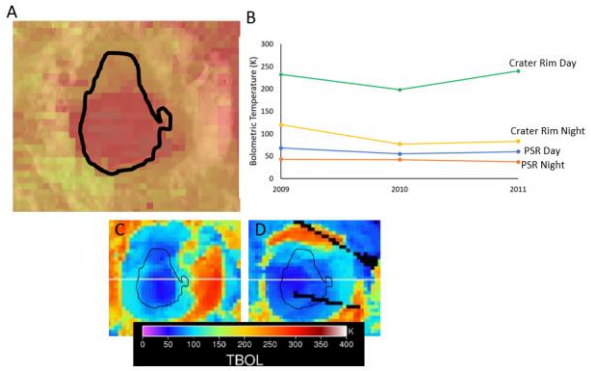

Figure 2: de Gerlache crater with PSR outlined in black. A) LOLA albedo overlain on LROC imaging. B) Averaged Diviner data from 2009-2011 (Green – Crater rim/wall temperature; Blue – PSR Daytime; Gold – Crater rim/wall; Red – PSR Nighttime) . C) Daytime bolometric temperature from Diviner. D) Nighttime bolometric temperature from Diviner.